Fluid Dynamics & Materials Processing

Tech Science Press

DOI: 10.32604/fdmp.2024.046360 Published Online: 20 March 2024

ARTICLE

An Investigation into the Performances of Cement Mortar Incorporating Superabsorbent Polymer Synthesized with Kaolin

Xiao Huang[1,2] and Jin Yang[3,*]

[1]State Key Laboratory of Featured Metal Materials and Life-Cycle Safety for Composite Structures, and School of Resources, Environment and Materials, Guangxi University, Nanning, 530004, China

[2]State Key Laboratory of Geomechanics and Geotechnical Engineering, Institute of Rock and Soil Mechanics, Chinese Academy of Sciences, Wuhan, 430071, China

[3]School of Civil Engineering, Architecture and Environment, Hubei University of Technology, Wuhan, 430068, China

[*]Corresponding Author: Jin Yang. Email: jinyang@hbut.edu.cn

Received: 27 September 2023 Accepted: 28 December 2023

ABSTRACT

Cement-based materials are fundamental in the construction industry, and enhancing their properties is an ongoing challenge. The use of superabsorbent polymers (SAP) has gained significant attention as a possible way to improve the performance of cement-based materials due to their unique water-absorption and retention properties. This study investigates the multifaceted impact of kaolin intercalation-modified superabsorbent polymers (K-SAP) on the properties of cement mortar. The results show that K-SAP significantly affects the cement mortar's rheological behavior, with distinct phases of water absorption and release, leading to changes in workability over time. Furthermore, K-SAP alters the hydration kinetics, delaying the exothermic peak of hydration and subsequently modifying the heat release kinetics. Notably, K-SAP effectively maintains a higher internal relative humidity within the mortar, reducing the autogenous shrinkage behavior. Moreover, K-SAP can have a beneficial effect on pore structure and this can be ascribed to the internal curing effect of released water from K-SAP.

KEYWORDS

Superabsorbent polymer; kaolin; cement mortar; rheological behavior; autogenous shrinkage

1 Introduction

With the extensive application of concrete in the infrastructure development, concerns arise regarding factors like a low water-cement ratio and the overuse of admixtures. These factors can result in inadequate moisture levels within the concrete, making it highly vulnerable to premature self-drying. Consequently, this susceptibility leads to the development of excessive internal stress and the formation of microcracks within the cement matrix, ultimately contributing to early cracking. The approach of internal curing techniques [1–3] primarily involves the incorporation of internal curing materials to address the challenges associated with low water-cement ratio cementitious materials. By employing internal curing [4], additional water is introduced into the concrete, effectively maintaining relative

humidity within the cementitious material. This process mitigates the issues of self-drying and cracking, serving to compensate for shrinkage and enhance the overall durability of the concrete structure.

In 2002, researchers proposed the utilization of materials [5] as an agent [6] for internal curing, aligning with advancements in materials science. Superabsorbent polymers (SAP) represent organic substances with the unique ability to absorb water and gradually form a three-dimensional network. Their distinctive properties include the capacity to absorb several hundred to thousand times their own weight in solution, demonstrating high water absorption and retention capabilities. Once absorbed, moisture is predominantly stored within the resin network, indicating a process of physical adsorption within the polymer matrix. SAP, characterized by a macroscopic gel structure with cross-linked networks, can absorb substantial quantities of water from the environment and dissolve molecules present in the surrounding air, resulting in the formation of a saturated gel. Consequently, SAP exhibits attributes of an elastic gel. Its capacity to absorb moisture from the surrounding air and undergo swelling allows for responses to changes in pH or the concentration of specific ions in the environment, triggering the controlled release of water.

SAP exhibits the ability to release free water within concrete during periods of reduced humidity. This liberated water plays a crucial role in curing the hydration of cementitious materials, effectively mitigating autogenous shrinkage and thereby preventing cracking induced by this phenomenon [7,8]. Notably, when compared to alternative internal curing agents like lightweight aggregates, SAP demonstrates superior internal curing efficiency while imposing minimal adverse effects on strength. Despite the introduction of voids within concrete upon water release, the uniformly distributed SAP voids contribute to mitigating the quality and dynamic modulus loss of concrete during freeze-thaw cycles, thereby enhancing its frost resistance [9,10]. In contrast to air-entraining agents, the pore system associated with SAP remains more stable and undergoes insignificant changes during the processes of mixing and pumping. Furthermore, under external loads surpassing the concrete's bearing capacity, cracks tend to propagate along SAP voids. In conditions of high humidity, such as 90%, SAP located on crack surfaces has the capability to absorb moisture from the environment and subsequently release it into the matrix. This unique property accelerates the self-healing of cracks, promoting the restoration of mechanical and durability properties in pre-cracked concrete [11]. The distinct advantages of SAP make it a promising internal curing agent with multifaceted benefits for concrete performance.

Depending on the types of raw materials employed in their preparation, superabsorbent polymers (SAPs) can be broadly classified into starch-based, cellulose-based, and synthetic-based categories. Within the synthetic category, SAPs encompass variations such as the acrylic acid (AA) series [12,13], acrylamide (AM) series [14–16], or copolymers combining both (AA-AM) [17–21]. Despite the existence of numerous SAP types with subtle distinctions, many of them have not yet been explored for potential applications in concrete internal curing. In certain instances, researchers have introduced inorganic intercalating materials, such as montmorillonite, into the three-dimensional cross-linked network structure of SAP to enhance specific properties like water absorption capacity, salt resistance, and elastic modulus. Inorganic intercalating materials possess a layered structure, facilitating their incorporation into polymers to create layered composite materials. Common examples of these materials include graphite, montmorillonite, kaolin, and others, all of which have demonstrated satisfactory enhancements to the engineering properties of cement-based materials [22]. Despite this, research on the synthesis and the effects of inorganic intercalating material-modified SAP on the properties and microstructure of cementitious materials has been relatively limited. Further exploration in this area holds the potential to uncover novel approaches for improving and tailoring the performance of SAPs in concrete applications.

This study involved the synthesis and preparation of kaolin intercalation-modified superabsorbent polymers, utilizing acrylic acid and acrylamide as monomers, with kaolin serving as the inorganic intercalating material. The study systematically explored the influence of kaolin-modified superabsorbent polymers on various aspects of cement mortar, including rheological properties, heat of hydration, mechanical properties, internal relative humidity, autogenous shrinkage, and pore structure. Given the

fixed water-to-cement ratio of 0.35 in this study, autogenous shrinkage within the matrix assumes a predominant role compared to drying shrinkage [23]. Consequently, the investigation focuses exclusively on assessing the impact of superabsorbent polymers on autogenous shrinkage.

2 Materials and Methods

2.1 Materials

The SAP synthesized in this study primarily consisted of acrylic acid and acrylamide as monomers, with recycled kaolin clay used as an intercalation-modifying material. The recycled kaolin clay is provided by the commercial company. N,N′-methylenebisacrylamide served as the cross-linking agent, and potassium persulfate ($K_2S_2O_8$) as the initiator. Portland Type I 52.5 cement was employed in this study, and its composition is presented in Table 1, with a median particle size of 17.8 μm. The fine aggregate used was natural river sand, with an approximate bulk density of 1460 kg/m^3. The admixture used was a polycarboxylate-based superplasticizer (PCE), which had a pale yellow color and a 40% solid content.

Table 1: Chemical composition of portland cement

CaO	SiO_2	Al_2O_3	Fe_2O_3	MgO	SO_3	Na_2O	Loss
65.12%	21.13%	4.12%	2.98%	1.53%	1.26%	1.24%	2.62%

2.2 Synthesis of Kaolin-Modified SAP

The SAP synthesis method employed in this investigation followed the sol–gel approach, with a specific preparation procedure outlined as follows: Initially, kaolin clay, constituting 10% of the monomer mass, was weighed and added to a mixture of acrylic acid and acrylamide (AA:AM = 4:1) solution. Ultrasonication was applied for dispersion. A combination of solid sodium hydroxide (NaOH) and deionized water was prepared. The clear NaOH solution was gradually introduced drop by drop into a beaker containing the acrylic acid solution, with the electric stirrer operating at a high speed. Concurrently, N,N′-methylenebisacrylamide (0.015% of the monomer mass) was added using weighing paper. Following the complete dissolution of the solution, potassium persulfate (0.25% of the monomer mass) was added and thoroughly mixed. Once the solution achieved clarity and uniformity, the beaker was placed in a constant-temperature water bath set at 65°C, and the formation of a gel-like substance was monitored with the stirrer in operation. Subsequently, after stopping the stirring, the beaker was transferred to an oven at 70°C for 1 h, and the resultant gel was cut into small pieces, placed in a Petri dish, and returned to the oven. After 48 h, the samples were retrieved, crushed, and ground into a powder using a grinder, which was then sealed in sample bags. Fig. 1 illustrates the physical appearance, infrared spectrum, and microscopic morphology of the kaolin-modified SAP powder (K-SAP). In the infrared spectrum (Thermo Scientific iN10, USA), stretching vibration peaks of CH_2 were observed at 2950 cm^{-1}, with vibration peaks at 1410 cm^{-1} and 1570 cm^{-1} indicating the presence of CH_3-(N^+). These results confirm the successful synthesis of K-SAP. Scanning electron microscopy (SEM, QUANTA250, USA) images revealed an irregular polyhedral morphology for the synthesized K-SAP, with a particle size ranging from 100 to 300 μm.

2.3 Cement Mortar Mix Proportions

The water-to-cement ratio (w/c) of the cement mortar was fixed at 0.35, and the cement-to-sand ratio (c/s) was fixed at 1:1, according to previous work [24]. An additional water-cement ratio of 0.063 was introduced, and the dosage of kaolin-modified SAP (K-SAP) was calculated based on the introduced water content and water absorption capacity. The water absorption capacity of K-SAP in the cement paste was determined using the flow table method, as described in Section 2.4. The cement mortar with the addition of kaolin-modified SAP was labeled as K-SAP, while the reference group mortar without SAP was labeled as Control.

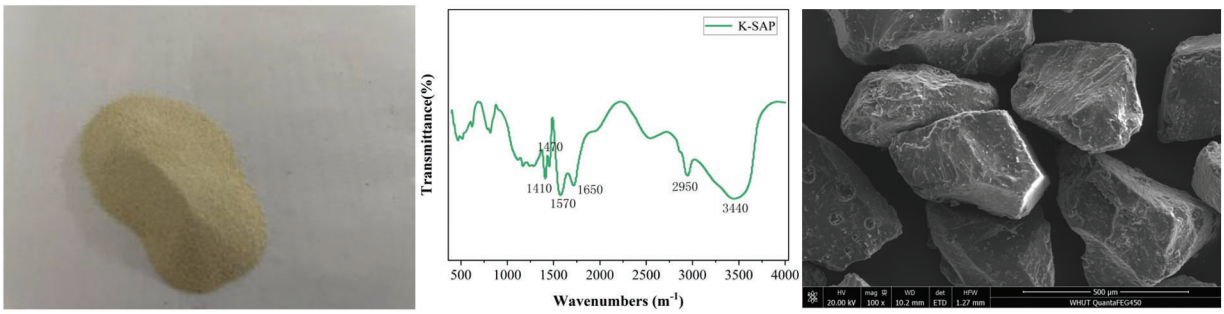

(a) Physicalphotograph (b) Infrared spectrum (c) SEM image

Figure 1: Physical photograph, infrared spectrum, and SEM image of K-SAP powder

2.4 Testing Methods

1. Water Absorption Capacity
   Initially, the cement paste underwent thorough mixing, and a wet cloth was employed to clean the glass plate and its mold. Subsequently, a circular mold was positioned at the center of the glass plate, and the cement paste was poured into it. A steel ruler was utilized to even the surface, and, after half a minute, the circular mold was lifted in the direction of gravity. The maximum diameter was measured, and the average value was computed as the flowability of the cement paste. This method provides a reliable assessment of the water absorption characteristics of K-SAP within the cementitious matrix.
2. Rheological Behavior
   Rheological behavior testing was conducted on cement paste with K-SAP using a touch-screen rheometer, with a speed range of 0.01–1300 RPM. Considering the influence of temperature on the rheological properties of paste samples, all measurements were conducted at a temperature of 20°C. Since the downward shear curve is more stable, this study selected the downward shear curve for analyzing the time-dependent rheological behavior of cement paste with the addition of K-SAP.
3. Hydration Heat
   A microcalorimeter was used for hydration heat testing in this study. The microcalorimeter has 8 channels, each with a sample chamber and a reference chamber, allowing for the simultaneous testing of 8 samples. The total mass of each formed specimen did not exceed 7 g. Analytical balances were used to accurately weigh the experimental raw materials to calculate the amount of hydration heat reference water. The testing temperature was maintained at 20°C, and the hydration heat testing duration was 3 days.
4. Compressive Strength
   Compressive strength tests for all cement mortar mixtures were conducted at 3 days, 7 days, and 28 days after curing. Cubic specimens measuring 40 mm × 40 mm × 40 mm were cast for each mortar mix. A layer of plastic film was used to cover the surface, and standard curing was carried out in a curing room at 20°C. After 24 h, the specimens were demolded, and immediately sealed with plastic film to prevent moisture exchange with the external environment.
5. Autogenous Shrinkage
   Cement mortar specimens with sizes of 40 mm × 40 mm × 160 mm were prepared. After standard curing for 24 h, the specimens were demolded and sealed with plastic film. It should be noted that the film was flat and not too thick, as excessive film thickness could affect the accuracy of the test results

by influencing the precision of the probe used. These sealed specimens were then securely placed on an automatic concrete shrinkage and expansion instrument, with the environmental temperature controlled at (20 ± 2)°C. Changes in specimen length were monitored using an electronic displacement probe attached to the cantilever arm. The electronic displacement probe made contact with the top of the specimen, and data was automatically collected by a built-in microcomputer in the instrument.

6. Internal Relative Humidity
   In this study, a triple mold with dimensions of 100 mm × 100 mm × 100 mm was used. Three specimens with the same mixture proportions were cast, and after mixing the cement mortar, a plastic pipe with a diameter of 20 mm and a length of 60 mm was inserted into each specimen to a depth of 50 mm as the testing channel. Longitudinal cuts were made on the plastic pipes to increase the contact area between the cement mortar and the probe, thereby enhancing the accuracy of the test. After molding, the specimens were placed in a curing room under standard conditions, and they were demolded after 24 h. A layer of plastic film was used to completely wrap the test specimens, and they were moved to the testing area. The testing probes were inserted into the plastic pipes and sealed with polyethylene tape to prevent air exchange between the interior of the specimens and the external environment. The temperature was maintained at 20°C, and data collection was conducted at 2-min intervals for a duration of 7 days.
7. Pore Structure
   Mercury intrusion porosimetry (MIP) is a commonly used method for testing the pore structure of cementitious materials, and it can measure pore sizes ranging from approximately 5 nm to 800 μm. A mercury intrusion test was performed on 28-day mortar specimens using a mercury porosimeter. Samples were taken from the central area of 28-day mortar specimens with a particle size of approximately 3 to 4 mm. These samples were dried in a drying oven at 50°C for 24 h to remove water from capillary pores. During the testing process, low-pressure testing (0.51 PSIA, equivalent to 3.52 kPa) was first conducted in the low-pressure chamber, followed by high-pressure testing (60000 PSIA, equivalent to 413.8 kPa) in the high-pressure chamber, with a contact angle of 130°.
8. Thermogravimetric Analysis
   Before testing, sealed and cured specimens were sampled after 28 days, and they were then immersed in ethanol to terminate hydration. Subsequently, the samples were ground into powder (approximately 3 to 5 g) and dried at 60°C for 24 h. The ground powder was tested using a comprehensive thermal analyzer. Nitrogen gas was introduced, and the sample was heated from room temperature to 1000°C at a heating rate of 10°C/min with a flow rate of 15 mL/min.

3 Results and Discussion

3.1 Rheological Behavior

The time-dependent influence of K-SAP on the rheological behavior of cement paste is illustrated in Fig. 2. The figure reveals that the shear stress in cement paste containing K-SAP initially decreases over time, reaching a turning point at 60 min, after which it exhibits an ascending trend. This behavior aligns with findings reported by Yang et al. [24]. Utilizing the Bingham model for analysis, it is determined that the cement paste with K-SAP displays shear-thinning behavior. The time-dependent rheological curve of the cement paste suggests that changes in rheological behavior are linked to the rate of water release from K-SAP and moisture consumption during cement hydration. These changes manifest in two stages: The first stage is the rapid water release phase of SAP, primarily occurring during the initial period up to 60 min. As cement hydration progresses, the total ion concentration in the paste increases, resulting in a

substantial osmotic pressure difference. This prompts continuous water release from K-SAP into the cement matrix. The rate of water release surpasses the rate of moisture consumption, leading to a decrease in yield stress due to the greater impact of K-SAP water release compared to the increase in shear stress caused by cement hydration. The second stage occurs after 60 min, where K-SAP continues to release water into the cement mortar but at a rate slower than the moisture consumption rate. This implies ongoing thickening of the cement mortar, with cement hydration becoming the dominant factor in the increase in shear stress. Some studies have suggested that multiple experiments may impede the formation of hydration flocculation structures, and the use of highly efficient water reducers can contribute to a reduction in the initial yield stress [25].

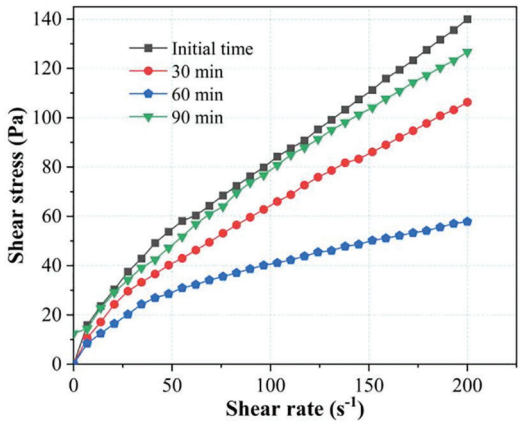

Figure 2: Time-dependent influence of K-SAP on the rheological behavior of cement paste

3.2 Hydration Heat

Fig. 3 illustrates the impact of K-SAP on the hydration heat release rate and cumulative heat release of cement paste. In Fig. 3a, it is evident that the heat release rate of cement paste, with and without K-SAP, shows similarity before the induction period. However, the introduction of K-SAP leads to a noticeable reduction in the heat release rate during the acceleration period of the cementitious material system, coupled with a delayed heat release peak. Concurrently, the total heat release curve gradually converges with that of the reference group, as depicted in Fig. 3b. Between the 10–20 h, the decline in the heat release rate during the acceleration period with K-SAP may be attributed to the release of moisture stored by K-SAP. The water released by K-SAP increases the effective water-cement ratio of the cementitious material system, aligning with the established correlation between hydration heat and water-cement ratio in previous studies [26]. Additionally, some studies suggest that the reduction in the rate of heat release during the primary hydration peak may result from the absorption of alkaline ions, such as Ca^{2+}, by K-SAP. This absorption leads to the dilution of initial ion concentrations, thereby slowing down the hydration reaction [27,28]. Around the 16-h mark, the heat release rate of the cement mortar surpasses that of the reference group. This is attributed to the fact that during the deceleration period, the addition of K-SAP supplies water to the cement after the hydration reaction. This water supply prolongs the hydration reaction time and ensures a more complete cement hydration reaction [29,30]. This observation also elucidates why the total heat release curve of K-SAP in Fig. 3b is lower than that of the reference group, indicating that some of the SAP moisture remains unreleased at 72 h.

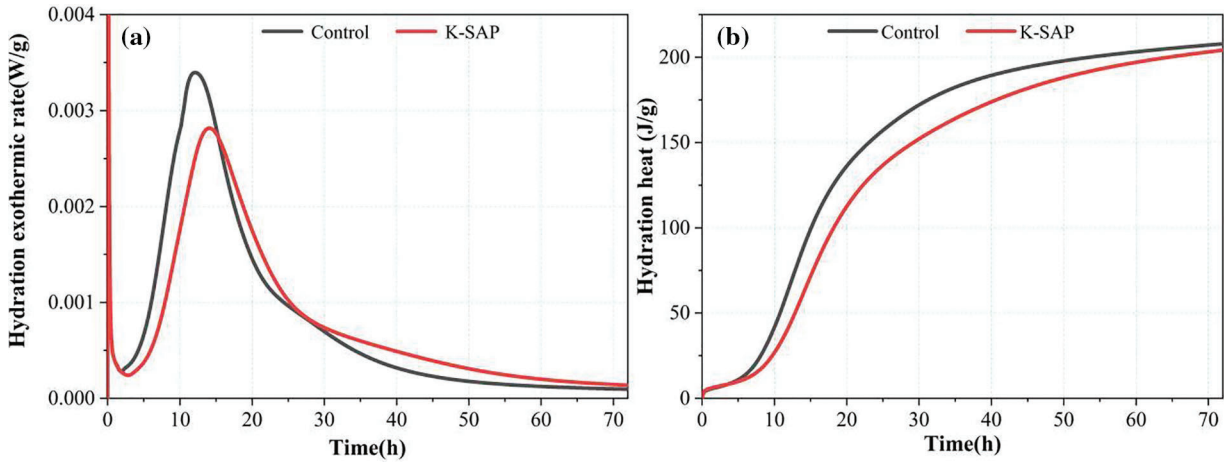

Figure 3: Influence of K-SAP on the hydration heat of cement paste

3.3 Thermal Analysis

Fig. 4 displays the thermal gravimetric curve of K-SAP hardened cement paste. In Fig. 4a, a noticeable distinction is observed in the total mass loss rate of K-SAP compared to the reference group as the temperature increases, with a maximum difference of 7%. Analyzing the DTG curve in Fig. 4b, it becomes apparent that the weight loss peaks in the K-SAP group are significantly higher than those in the reference group within temperature ranges of 60°C–200°C, 400°C–450°C, and 600°C–650°C. The mass loss within the 60°C–200°C range is primarily attributed to the removal of free water, physically bound water, and the dehydration of C-S-H gel. The high-alumina clay in K-SAP contains hydroxyl hydrophilic functional groups that form bound water through hydrogen bonds with water. Moreover, K-SAP facilitates additional hydration of the cement paste, leading to the formation of more C-S-H gel. The weight loss peak within the 400°C–450°C range is mainly associated with the decomposition of $Ca(OH)_2$ [27], providing further evidence of a heightened degree of hydration in the K-SAP group compared to the reference group [31]. The weight loss peak within the 600°C–650°C range corresponds to the decomposition of calcium carbonate, indicating that carbonation during the curing process transforms $Ca(OH)_2$ into calcium carbonate. This observation further suggests that K-SAP promotes the hydration of the cement mortar [25].

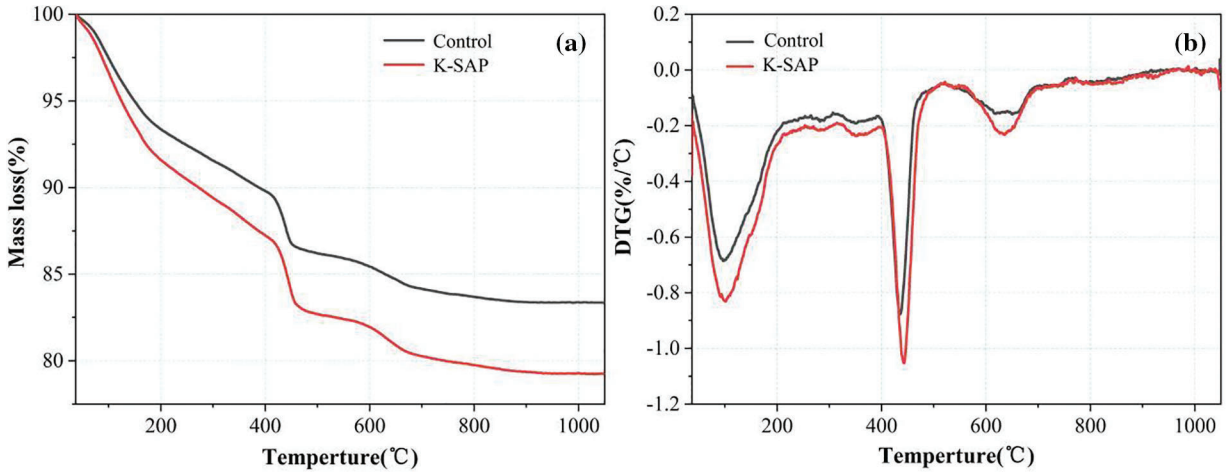

Figure 4: Thermal gravimetric curve of hardened cement paste with K-SAP

3.4 Compressive Strength

The influence of K-SAP on the compressive strength of cement mortar is depicted in Fig. 5. The figure illustrates a notable adverse effect associated with the addition of K-SAP on the compressive strength of the cement mortar. Across various ages, the compressive strength of the K-SAP-modified specimens exhibits a consistent declining trend. At 3 days, the strength of the reference group measures approximately 56 MPa, while the K-SAP-modified specimens achieve only about 71.4% of the strength of the reference group. This disparity diminishes to 75% at 7 days, and by 28 days, the strength improvement becomes more apparent, with the K-SAP group reaching around 60 MPa, equivalent to 85% of the reference group's strength, thereby narrowing the gap between them. In a study by Wang et al. [32], the synthesis of metakaolin/P(AA-co-AM) composite SAP, based on modified metakaolin, similarly resulted in approximately a 20% reduction in the 28 days compressive strength relative to the reference group in cement mortar.

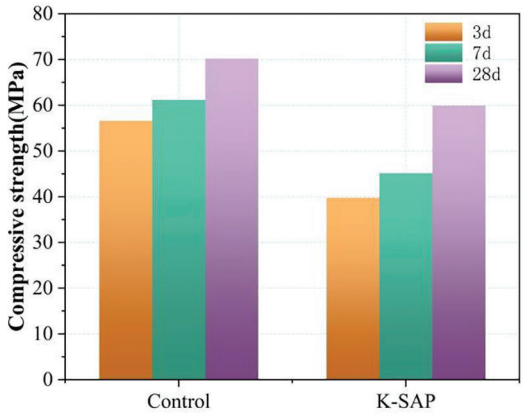

Figure 5: Influence of K-SAP on the compressive strength of cement mortar

The decline in compressive strength observed in the K-SAP-incorporated group can be attributed to several contributing factors. Firstly, K-SAP absorbs water and undergoes swelling within the cement mortar. Throughout the cement hydration process, it consistently releases water to supplement the required hydration, resulting in volume shrinkage and the creation of numerous voids within the cement mortar. This inherently diminishes its own strength [25,29,33]. Secondly, during the initial water-release stage, K-SAP proportionately raises the effective water-cement ratio in the interfacial transition zone. It is widely acknowledged that the compressive strength of cement mortar is directly correlated to the water-cement ratio. Consequently, as the water-cement ratio increases, the compressive strength of the cement mortar decreases [34,35]. The combined influence of these two factors leads to a substantial reduction in compressive strength during the early stages. As the curing time progresses, the strength disparity between the K-SAP-incorporated group and the reference group gradually diminishes. Two main reasons account for this phenomenon. Firstly, K-SAP can sustain the relative humidity within the cement mortar, facilitating more comprehensive cement hydration. This results in a denser interfacial transition zone between K-SAP and the cement mortar [30]. Secondly, the elevated alumina content in K-SAP implies its capacity to react with ions such as Ca^{2+} present in the cement mortar, generating hydration products that can partially fill the voids left by SAP [31,35,36]. This ultimately leads to an augmentation in compressive strength in the later stages, aligning with findings from previous research [29].

3.5 Internal Relative Humidity

The influence of K-SAP on the internal relative humidity of cement mortar is illustrated in Fig. 6. The graph clearly indicates that the internal relative humidity of the cement mortar in the K-SAP incorporated

group is markedly higher than that in the reference group. This advantage becomes more pronounced as the hydration process advances. Around 12,000 min, the internal relative humidity in the K-SAP group exhibits minimal decrease, while the reference group experiences a decline from an initial 92% relative humidity to 87% relative humidity. This observation signifies the effective ability of K-SAP to maintain internal relative humidity within the cement matrix.

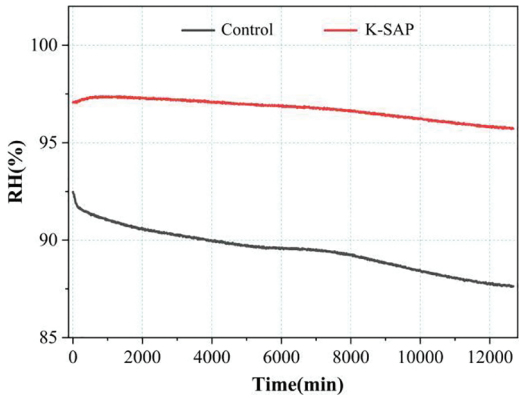

Figure 6: Influence of K-SAP on internal relative humidity of cement mortar

As is well-known, the hydration of cement is an ongoing process that entails the continuous consumption of water, inevitably resulting in a decline in its internal relative humidity. In the case of the reference group, during the initial stages, its internal relative humidity curve experiences a rapid drop, indicating the swift utilization of water in the initial phases of cement hydration. Notably, during this phase, the internal relative humidity in the K-SAP group remains nearly constant. This can be primarily attributed to the exceptional water-retaining properties of K-SAP, which serves as a modified internal curing agent within the cement matrix. Throughout the cement hydration process, K-SAP operates as a reservoir, consistently releasing entrapped internal curing water into the surrounding cementitious matrix due to humidity gradients [37] and osmotic pressure [38]. This continuous release, in turn, sustains a high level of relative humidity within the internal environment of the cementitious matrix for an extended duration [39,40].

3.6 Autogenous Shrinkage

The effect of K-SAP on the autogenous shrinkage of cement mortar is depicted in Fig. 7. As shown in the figure, the incorporation of K-SAP leads to a substantial reduction in the autogenous shrinkage of the mortar. In comparison to the reference group, the K-SAP group demonstrates a reduction of 68.75%.

While autogenous shrinkage in cement mortar results from the interplay of various factors, its primary cause lies in the rapid reduction of internal relative humidity. In the initial stages, as moisture diminishes swiftly, capillary pores gradually occupy spaces previously held by water. The water within these capillary pores generates capillary pressure in the cementitious matrix due to surface tension, resulting in the compression of the cementitious matrix. This compression is visually observed as a volumetric reduction [41]. Theoretically, cement-based materials with a low water-to-cement ratio undergo substantial volume shrinkage due to insufficient water for complete hydration [42], explaining the significant autogenous shrinkage observed in the reference group. The integration of K-SAP significantly alleviates the autogenous shrinkage of the cement mortar matrix, primarily owing to its internal curing effects. Firstly, K-SAP, uniformly dispersed throughout the cement mortar, consistently compensates for the water consumed by cement hydration within the internal matrix, thereby decelerating the reduction in

the internal relative humidity of the cement mortar [43]. This ensures a sufficient moisture level in the capillaries, restraining the build-up of capillary pressure [44]. Secondly, the hydration products resulting from the reaction between high-alumina clay particles and calcium hydroxide can fill the voids left after water release, enhancing the overall stiffness of the cement mortar and reducing its overall shrinkage [29].

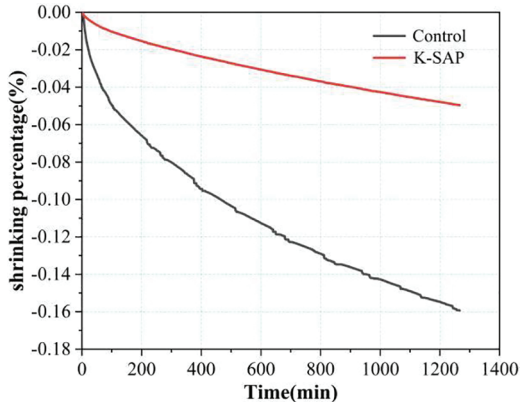

Figure 7: Influence of K-SAP on autogenous shrinkage of cement mortar

3.7 Pore Structure

The influence of K-SAP on the pore size distribution of cement mortar is depicted in Fig. 8. As shown in Fig. 8a, the cumulative intrusion volume in the large pore size range (above 6 μm) for the K-SAP group exhibits a significant increase compared to the reference group. Notably, Fig. 8b presents the micro-pore size distribution (below 20 nm), revealing that the number of pores with sizes between 10 and 20 nm is markedly higher in the K-SAP group than in the reference group. However, the number of pores with sizes smaller than 10 nm and those ranging from 20 to 100 nm is notably lower in the K-SAP group compared to the reference group.

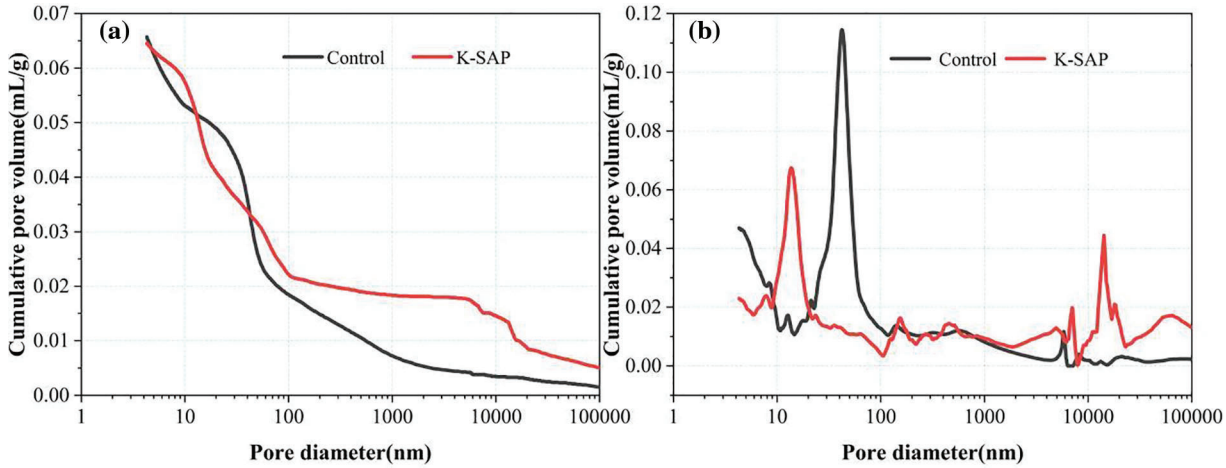

Figure 8: Influence of K-SAP on pore size distribution of cement mortar

In general, the pore structure of cement mortar can be classified into four types: gel pores (less than 10 nm), fine capillary pores (10–50 nm), medium capillary pores (50–100 nm), and macropores (greater than 100 nm) [45]. The results demonstrate that in the K-SAP group, the quantity of medium capillary

pores is significantly reduced, while the number of fine capillary pores and macropores is increased. This observation aligns with the findings of Li et al. [25]. The reasons are straightforward: K-SAP, acting as an internal curing agent, consistently releases water during the cement mortar hydration process, promoting internal hydration of the cement mortar. Additionally, the inorganic active particles in kaolin clay, through reactions with Ca^{2+} in the cementitious matrix, generate hydration products such as C-S-H gel, further densifying the pore structure [25,29]. These two factors collaborate to optimize the pore structure, specifically transforming medium capillary pores into fine capillary pores and fine capillary pores into gel pores. The increase in macropores in the K-SAP group is primarily due to the voids left by K-SAP as it releases water, and its rapid water release elevates the effective water-to-cement ratio in the cement matrix, leading to the formation of diffusion pores and increasing the proportion of capillary pores [46]. The addition of K-SAP significantly raises the proportion of macropores (greater than 100 nm), which are detrimental to mechanical performance, constituting a significant reason for the reduction in the compressive strength of the matrix. Furthermore, the incorporation of K-SAP also results in a substantial decrease in the number of capillary pores (less than 100 nm), effectively reducing capillary pressure in the matrix and contributing to a noteworthy reduction in autogenous shrinkage.

4 Conclusions

In this study, the influence of K-SAP on various properties of cement mortar has been comprehensively investigated. The conclusions can be drawn from the experimental results as below:

1. The incorporation of K-SAP induced notable changes in the rheological behavior of cement mortar. Initially, K-SAP led to a reduction in shear stress, followed by a subsequent increase, indicative of shear-thinning behavior. This behavior is attributed to the rapid water release from K-SAP and its role in elevating the water-to-cement ratio.

2. K-SAP exerted a significant influence on the hydration process of cement mortar. It effectively reduced early-stage heat release, delaying the occurrence of the hydration heat peak. This delay in peak hydration heat can be attributed to K-SAP's water-retaining capacity, leading to the dilution of ionic concentration in the mortar.

3. Thermal analysis highlighted differences in weight loss peaks during the hydration process, indicating enhanced hydration reactions in the presence of K-SAP. The addition of K-SAP initially led to a decrease in compressive strength due to water absorption and swelling, causing void formation. However, with prolonged curing time, the strength difference between the K-SAP-added mortar and the control group diminished.

4. K-SAP induced changes in the pore structure of cement mortar. It increased the pore volume of macropores and fine capillary pores while decreasing medium capillary pores. This transformation optimally modified the pore structure, contributing to the overall densification of the mortar.

Acknowledgement: The authors would like to take this opportunity to express our heartfelt gratitude to all who have assisted us.

Funding Statement: This research was funded by the National Natural Science Foundation of China (52172017 and 51902095).

Author Contributions: The authors confirm their contribution to the paper as follows: Study conception and design: Jin Yang; data collection: Xiao Huang; analysis and interpretation of results: Jin Yang; draft manuscript preparation: Xiao Huang. All authors reviewed the results and approved the final version of the manuscript.

Availability of Data and Materials: Data will be made available on request.

Conflicts of Interest: The authors declare that they have no conflicts of interest to report regarding the present study.

References

1. Al Saffar, D. M., Al Saad, A. J. K., Tayeh, B. A. (2019). Effect of internal curing on behavior of high performance concrete: An overview. *Case Studies in Construction Materials, 10,* e00229.
2. El-Hawary, M., Al-Sulily, A. (2020). Internal curing of recycled aggregates concrete. *Journal of Cleaner Production, 275,* 122911.
3. Rasheed, L. S., Abdulrasool, A. T. (2020). Recyclable wastes as internal curing materials to improve high-performance concrete's sustainability, and durability: An overview. *IOP Conference Series: Materials Science and Engineering, 928(2),* 22071.
4. Kiran, V. K., Chary, T. K., Jayaram, M., Sindhu, B. (2021). A novel approach on properties of internal curing concrete and impact of salts. *IOP Conference Series: Materials Science and Engineering, 1057(1),* 12078.
5. Siramanont, J., Vichit-Vadakan, W., Siriwatwechakul, W. (2010). The impact of SAP structure on the effectiveness of internal curing. *International RILEM Conference on Use of Superabsorbent Polymers and Other New Additives in Concrete*, France, RILEM Publications SARL Bagneux.
6. Li, Z., Zhang, S., Liang, X., Granja, J., Azenha, M. et al. (2020). Internal curing of alkali-activated slag-fly ash paste with superabsorbent polymers. *Construction and Building Materials, 263,* 120985.
7. Kang, S. H., Hong, S. G., Moon, J. (2017). Absorption kinetics of superabsorbent polymers (SAP) in various cement-based solutions. *Cement and Concrete Research, 97,* 73–83.
8. Schröfl, C., Erk, K. A., Siriwatwechakul, W., Wyrzykowski, M., Snoeck, D. (2022). Recent progress in superabsorbent polymers for concrete. *Cement and Concrete Research, 151,* 106648.
9. Laustsen, S., Hasholt, M. T., Jensen, O. M. (2015). Void structure of concrete with superabsorbent polymers and its relation to frost resistance of concrete. *Materials and Structures, 48(1),* 357–368.
10. Mechtcherine, V., Schröfl, C., Wyrzykowski, M., Gorges, M., Lura, P. et al. (2017). Effect of superabsorbent polymers (SAP) on the freeze-thaw resistance of concrete: Results of a RILEM interlaboratory study. *Materials and Structures, 50(1),* 14.
11. Snoeck, D., van Tittelboom, K., Steuperaert, S., Dubruel, P., de Belie, N. (2012). Self-healing cementitious materials by the combination of microfibres and superabsorbent polymers. *Journal of Intelligent Material Systems and Structures, 25(1),* 13–24.
12. Jafari, M., Najafi, G. R., Sharif, M. A., Elyasi, Z. (2020). Superabsorbent polymer composites derived from polyacrylic acid: Design and synthesis, characterization, and swelling capacities. *Polymers and Polymer Composites, 29(6),* 733–739.
13. Wu, Z. G. (2008). *Research on the synthesis and modification of super absorbent resin (Master Thesis)*. Fourth Military Medical University, China.
14. Ma, L., Wang, J. H., Han, L., Lu, C. H. (2020). Preparation and research status of polyacrylamide. *Chemical Technology and Development, 49(11),* 39–42+71 (In Chinese).
15. Hemvichian, K., Chanthawong, A., Suwanmala, P. (2014). Synthesis and characterization of superabsorbent polymer prepared by radiation-induced graft copolymerization of acrylamide onto carboxymethyl cellulose for controlled release of agrochemicals. *Radiation Physics Chemistry, 103,* 167–171.
16. Foungfung, D., Phattanarudee, S., Seetapan, N., Kiatkamjornwong, S. (2011). Acrylamide-itaconic acid superabsorbent polymers and superabsorbent polymer/mica nanocomposites. *Polymers for Advanced Technologies, 22(5),* 635–647.
17. Anil, I., Gunday, S. T., Alagha, O., Bozkurt, A. (2019). Synthesis, characterization, and swelling behaviors of poly (acrylic acid-co-acrylamide)/pozzolan superabsorbent polymers. *Journal of Polymers the Environment, 27,* 1086–1095.

18. Khairkar, S., Raut, A. (2014). Chitosan-graft-poly(acrylicacid-co-acrylamide) superabsorbent hydrogel. *Journal of Chitin Chitosan Science, 2(4),* 288–292.
19. Mazlan, S., Abd Rahim, S., Ghazali, S., Jamari, S. S. (2022). Optimization of N, N′-methylenebis(acrylamide), and ammonium persulfate content in carbonaceous/acrylic acid-co-acrylamide superabsorbent polymer. *Materials Today: Proceedings, 57,* 1088–1094.
20. Schröfl, C. (2021). *Chemical design and synthesis of superabsorbent polymers*. Superabsorbent Polymers: Chemical Design, Processing, Applications.
21. Tang, G. (2011). *Research on the synthesis and performance of SA/P (AA/AM) interpenetrating polymer network super absorbent resin (Master Thesis)*. Anhui University, China.
22. Lang, L., Chen, B., Li, J. (2023). High-efficiency stabilization of dredged sediment using nano-modified and chemical-activated binary cement. *Journal of Rock Mechanics and Geotechnical Engineering, 15(8),* 2117–2131.
23. Tran, N. P., Gunasekara, C., Law, D. W., Houshyar, S., Setunge, S. et al. (2021). A critical review on drying shrinkage mitigation strategies in cement-based materials. *Journal of Building Engineering, 38,* 102210.
24. Yang, J., Wang, F., He, X., Su, Y., Wang, T. et al. (2021). Potential usage of porous autoclaved aerated concrete waste as eco-friendly internal curing agent for shrinkage compensation. *Journal of Cleaner Production, 320,* 128894.
25. Li, Y. F., Luo, H., Zhang, B., Wei, X., Wang, F. et al. (2023). Internal curing of natural hydraulic lime with superabsorbent polymers. *Materials Today Communications, 34,* 105064.
26. Lothenbach, B., Scrivener, K., Hooton, R. D. (2011). Supplementary cementitious materials. *Cement and Concrete Research, 41(12),* 1244–1256.
27. Lefever, G., Aggelis, D. G., De Belie, N., Raes, M., Hauffman, T. et al. (2020). The influence of superabsorbent polymers and nanosilica on the hydration process and microstructure of cementitious mixtures. *Materials, 13(22),* 5194.
28. Justs, J., Wyrzykowski, M., Winnefeld, F., Bajare, D., Lura, P. (2014). Influence of superabsorbent polymers on hydration of cement pastes with low water-to-binder ratio. *Journal of Thermal Analysis and Calorimetry, 115(1),* 425–432.
29. Sun, B. B., Wu, H., Song, W., Li, Z., Yu, J. (2020). Hydration, microstructure and autogenous shrinkage behaviors of cement mortars by addition of superabsorbent polymers. *Frontiers of Structural and Civil Engineering, 14(5),* 1274–1284.
30. Huang, X., Liu, X., Rong, H., Yang, X., Duan, Y. et al. (2022). Effect of super-absorbent polymer (SAP) incorporation method on mechanical and shrinkage properties of internally cured concrete. *Materials, 15(21),* 7854.
31. Zhang, G., Xia, H., Niu, Y., Song, L., Zhao, Y. et al. (2023). Microstructure refinement and affected zone reinforcement for internal curing cement paste by composite microgel with nano silica. *Cement and Concrete Composites, 138,* 105013.
32. Wang, K., Suining, Z., Rui, H., Peng, X. (2023). Effect of metakaolin/P (AA-co-AM) composite super absorbent polymer on properties of cement mortar. *Building Science, 39(9),* 131–139 (In Chinese).
33. Mechtcherine, V., Gorges, M., Schroefl, C., Assmann, A., Brameshuber, W. et al. (2014). Effect of internal curing by using superabsorbent polymers (SAP) on autogenous shrinkage and other properties of a high-performance fine-grained concrete: Results of a RILEM round-robin test. *Materials and Structures, 47(3),* 541–562.
34. Hasholt, M. T., Jensen, O. M., Kovler, K., Zhutovsky, S. (2012). Can superabsorent polymers mitigate autogenous shrinkage of internally cured concrete without compromising the strength? *Construction and Building Materials, 31,* 226–230.
35. Bose, B., Davis, C. R., Erk, K. A. (2021). Microstructural refinement of cement paste internally cured by polyacrylamide composite hydrogel particles containing silica fume and nanosilica. *Cement and Concrete Research, 143,* 106400.
36. Vafaei, B., Farzanian, K., Ghahremaninezhad, A. (2021). Effect of hydrogels containing nanosilica on the properties of cement pastes. *Journal of Composites Science, 5(4),* 105.

37. He, X., Yang, J., Niu, M., Zhang, G., Li, G. (2023). Study on expansion effect and hydration characteristics of ultra-high strength cement-based grouting materials based on humidity compensation. *Case Studies in Construction Materials, 18,* e01941.
38. Yang, J., Wang, F. Z., Liu, Z. C., Liu, Y. P., Hu, S. G. (2019). Early-state water migration characteristics of superabsorbent polymers in cement pastes. *Cement and Concrete Research, 118,* 25–37.
39. Liu, C., Shen, D., Li, M., Li, C., Kang, J. et al. (2023). Investigation on the internal relative humidity of superabsorbent polymer-modified concrete exposed to various ambient humidities at early age. *Journal of Materials in Civil Engineering, 35(4),* 04023047.
40. Shen, D., Li, C., Li, M., Liu, C., Kang, J. (2022). Experimental investigation on correlation between autogenous shrinkage and internal relative humidity of superabsorbent polymer-modified concrete. *Journal of Materials in Civil Engineering, 34(2),* 04021456.
41. Yang, J., Huang, J., He, X., Su, Y., Oh, S. K. (2020). Shrinkage properties and microstructure of high volume ultrafine phosphorous slag blended cement mortars with superabsorbent polymer. *Journal of Building Engineering, 29,* 101121.
42. Hasselman, D. P. H. (1969). Griffith flaws and the effect of porosity on tensile strength of brittle ceramics. *Journal of the American Ceramic Society, 52(8),* 457.
43. Farzanian, K., Ghahremaninezhad, A. (2018). Desorption of superabsorbent hydrogels with varied chemical compositions in cementitious materials. *Materials and Structures, 51(1),* 1–15.
44. Snoeck, D., Jensen, O. M., de Belie, N. (2015). The influence of superabsorbent polymers on the autogenous shrinkage properties of cement pastes with supplementary cementitious materials. *Cement and Concrete Research, 74,* 59–67.
45. Yang, J., Hu, H., He, X., Su, Y., Wang, Y. et al. (2021). Effect of steam curing on compressive strength and microstructure of high volume ultrafine fly ash cement mortar. *Construction and Building Materials, 266,* 120894.
46. Jiang, D. B., Li, X., Lv, Y., Li, C., Jiang, W. et al. (2021). Autogenous shrinkage and hydration property of alkali activated slag pastes containing superabsorbent polymer. *Cement and Concrete Research, 149,* 106581.